



**SURVIVABILITY • SUSTAINABILITY • MOBILITY
SCIENCE AND TECHNOLOGY
SOLDIER SYSTEM INTEGRATION**



**TECHNICAL REPORT
NATICK/TR-96/029**

AD _____

THE MATHEMATICAL FOUNDATION AND THE BOUNDARY CONDITIONS ENCOUNTERED IN LASER ENERGY DIFFUSION IN A SOLID AND SKIN SIMULANT TEMPERATURE RISE

**By
Chia Ping Wang**

June 1996

**FINAL REPORT
November 1994 - October 1995**

Approved for Public Release; Distribution Unlimited

**U.S. ARMY SOLDIER SYSTEMS COMMAND
NATICK RESEARCH, DEVELOPMENT AND ENGINEERING CENTER
NATICK, MASSACHUSETTS 01760-5019
SURVIVABILITY DIRECTORATE**

19960617 111

DTIC QUALITY INSPECTED 1

DISCLAIMERS

The findings contained in this report are not to be construed as an official Department of the Army position unless so designated by other authorized documents.

Citation of trade names in this report does not constitute an official endorsement or approval of the use of such items.

DESTRUCTION NOTICE

For Classified Documents:

Follow the procedures in DoD 5200.22-M, Industrial Security Manual, Section II-19 or DoD 5200.1-R, Information Security Program Regulation, Chapter IX.

For Unclassified/Limited Distribution Documents:

Destroy by any method that prevents disclosure of contents or reconstruction of the document.

REPORT DOCUMENTATION PAGE			Form Approved OMB No. 0704-0188	
Public reporting burden for this collection of information is estimated to average 1 hour per response, including the time for reviewing instructions, searching existing data sources, gathering and maintaining the data needed, and completing and reviewing the collection of information. Send comments regarding this burden estimate or any other aspect of this collection of information, including suggestions for reducing this burden, to Washington Headquarters Services, Directorate for Information Operations and Reports, 1215 Jefferson Davis Highway, Suite 1204, Arlington, VA 22202-4302, and to the Office of Management and Budget, Paperwork Reduction Project (0704-0188), Washington, DC 20503.				
1. AGENCY USE ONLY (Leave blank)		2. REPORT DATE June 1996	3. REPORT TYPE AND DATES COVERED FINAL Nov 1994 - Oct 1995	
4. TITLE AND SUBTITLE THE MATHEMATICAL FOUNDATION AND THE BOUNDARY CONDITIONS ENCOUNTERED IN LASER ENERGY DIFFUSION IN A SOLID AND SKIN SIMULANT TEMPERATURE RISE			5. FUNDING NUMBERS AH98CA0B00	
6. AUTHOR(S) Chia Ping Wang				
7. PERFORMING ORGANIZATION NAME(S) AND ADDRESS(ES) U.S. Army Soldier Systems Command (SSCOM) Natick Research, Development and Engineering Center Kansas St. ATTN: SSCNC-IT Natick, MA 01760-5019			8. PERFORMING ORGANIZATION REPORT NUMBER NATICK/TR-96/029	
9. SPONSORING / MONITORING AGENCY NAME(S) AND ADDRESS(ES)			10. SPONSORING / MONITORING AGENCY REPORT NUMBER	
11. SUPPLEMENTARY NOTES				
12a. DISTRIBUTION / AVAILABILITY STATEMENT Approved for public release; distribution unlimited			12b. DISTRIBUTION CODE	
13. ABSTRACT (Maximum 200 words) The energy diffusion from a laser beam in a solid was critically analyzed and the solutions were applied to the problem of temperature rise of a skin simulant irradiated with a laser beam. The solutions involved two sets of contradicting boundary conditions: The zero surface heat flux vs the constant surface heat flux at the boundary. It is shown that the constant surface heat flux boundary condition in the conventional solution of the diffusion equation is unrealistic for a laser beam. Justification for the zero surface heat flux boundary condition for laser irradiation is presented along with the calculations for the temperature rise of a laser irradiated skin simulant. For laser exposures of 1000, 400, 100, 50 and 20 uS, the values of the surface temperature rise given by the constant surface heat flux solutions are higher by a factor of 2.2, 2.8, 4.9, 6.6 and 9.8, respectively, than that given by the zero surface heat flux solution. The analysis holds for the general case of other irradiated solids.				
14. SUBJECT TERMS LASER ENERGY DIFFUSION HEAT FLUX SKIN SIMULANT BOUNDARY CONDITIONS LASER IRRADIATION THERMAL DIFFUSION LASER APPLICATIONS EYE PROTECTION			15. NUMBER OF PAGES 27	
			16. PRICE CODE	
17. SECURITY CLASSIFICATION OF REPORT UNCLASSIFIED	18. SECURITY CLASSIFICATION OF THIS PAGE UNCLASSIFIED	19. SECURITY CLASSIFICATION OF ABSTRACT UNCLASSIFIED	20. LIMITATION OF ABSTRACT SAR	

Table of Contents

List of Figures	v
List of Tables	vii
Preface	ix
Acknowledgements	ix
1. Introduction	1
2. Thermal Diffusion and Boundary Conditions	1
3. Boundary Conditions for an Irradiating Laser Beam	3
4. The Zero Surface Heat Flux Solution	4
5. Computations for a Skin Simulant - Long Duration Laser Pulse	5
6. Millisecond and Microsecond Laser Pulses - Difference in the Two Formulations and the Depths of Penetration	8
7. Discussion	15
8. Conclusions	18
References	19

LIST OF FIGURES

1. Temperature rise curves of skin simulant exposed to a laser pulse of $\tau = 10\text{s}$, $\phi_0 = 0.167 \text{ cal cm}^{-2} \text{ s}^{-1}$ at depths $x = 0, 40, 80, 120$ and $160 \text{ }\mu\text{M}$ 6
2. Temperature rise curves of skin simulant exposed to a laser pulse of $\tau = 0.5\text{s}$, $\phi_0 = 0.167 \text{ cal cm}^{-2} \text{ s}^{-1}$ at depths $x = 0, 40, 80, 120$ and $160 \text{ }\mu\text{M}$ 7
3. Temperature rise of skin simulant at depths $x = 0, 40$, and $80 \text{ }\mu\text{M}$ for laser exposure of $\tau = 1\text{ms}$, $\phi_0 = 40$ and $16.7 \text{ cal cm}^{-2} \text{ s}^{-1}$. Heavy lines are with $\partial T/\partial x|_{x=0}=0$, light lines with $-K\partial T/\partial x|_{x=0} = \phi_0$ boundary conditions. The figure shows the much higher surface temperature rise of a solid given by the constant surface heat flux solution. 10
4. Temperature rise of a skin simulant at depths $x = 0, 40$, and $80 \text{ }\mu\text{M}$ for laser exposure of $\tau = 400 \text{ }\mu\text{s}$, $\phi_0 = 40$ and $16.7 \text{ cal cm}^{-2} \text{ s}^{-1}$. The figure shows the much higher surface temperature rise of a solid given by the constant surface heat flux solution. 11
5. Temperature rise of a skin simulant at depths $x = 0, 40$, and $80 \text{ }\mu\text{M}$ for laser exposure of $\tau = 100 \text{ }\mu\text{s}$, $\phi_0 = 40$ and $16.7 \text{ cal cm}^{-2} \text{ s}^{-1}$. The figure shows the much higher surface temperature rise of a solid given by the constant surface heat flux solution. 12
6. Temperature rise of a skin simulant at depths $x = 0, 40$, and $80 \text{ }\mu\text{M}$ for laser exposure of $\tau = 50 \text{ }\mu\text{s}$, $\phi_0 = 40$ and $16.7 \text{ cal cm}^{-2} \text{ s}^{-1}$. The figure shows the much higher surface temperature rise of a solid given by the constant surface heat flux solution. 13
7. Temperature rise of a skin simulant at depths $x = 0, 40$, and $80 \text{ }\mu\text{M}$ for laser exposure of $\tau = 20 \text{ }\mu\text{s}$, $\phi_0 = 40$ and $16.7 \text{ cal cm}^{-2} \text{ s}^{-1}$. The figure shows the much higher surface temperature rise of a solid given by the constant surface heat flux solution. 14

LIST OF TABLES

1. Temperature peaks at various depths of skin simulant exposed to laser pulse of $\tau = 0.5\text{s}$ and $\phi_0 = 0.167 \text{ cal cm}^{-2}\text{s}^{-1}$	8
2. Temperature rise by two Different Boundary Conditions, $\phi_0 = 40 \text{ cal cm}^{-2}\text{s}^{-1}$	16
3. Temperature rise by two Different Boundary Conditions, $\phi_0 = 16.7 \text{ cal cm}^{-2}\text{s}^{-1}$	17

PREFACE

The author was very much attracted by the very fine and intense beam of the laser when he was working on a laser interferometer in collaboration with Prof. Otto R. Frisch at the Cavendish Laboratory, University of Cambridge, for a bubble chamber particle track measuring device, the SWEEPNIK. The very fine beam enabled the track measurement to be accurate to a few microns. Later, high power lasers were used for welding and cutting, and in the study of thermal nuclear fusion. The diffusion of beam energy plays the central role in all these applications. The diffusion of beam energy comes into the picture again in the study of skin burn and eye damage by lasers. This report concerns the basic questions regarding the boundary condition of energy diffusion which seems to be the key to understand the great variety of diffusion phenomena. A great deal of time has been spent to program and properly run the newly installed mainframe computer at Natick for scientific computing. The work was funded as AH98CA0B00, Thermal Protection , covering the period from November 1994 to October 1995. Programs written previously were most helpful.

ACKNOWLEDGEMENTS

The author would like to thank his colleagues in the laser team at the US Army Soldier Systems Command, Natick Research Development and Engineering Center, for their interest and discussion and the assistance given him in preparing the text file in SCIENTIFIC WORK during the secretarial transfer/training.

THE MATHEMATICAL FOUNDATION AND THE BOUNDARY CONDITIONS ENCOUNTERED IN LASER ENERGY DIFFUSION IN A SOLID AND SKIN SIMULANT TEMPERATURE RISE

1. Introduction

The diffusion of energy from a laser beam is a very important process in laser physics and relates to a great many areas of application of a laser, from the protection of skin and eye of personnel against such radiation and the many applications in medical science of a low energy laser, to laser welding, laser cutting and the like by a high power laser, not to mention the role the energy diffusion plays in the very high power laser-induced thermal nuclear fusion.

As the diffusion of beam energy relates to so many areas of laser applications, the problem was critically analyzed, and the solutions were calculated for a skin simulant exposed to laser radiation with exposures ranging from 10 seconds to 20 microseconds.

As will be seen in the following sections, the solutions involve two sets of boundary conditions which are contradicting to each other. This then leads to the fundamental questions regarding the boundary conditions of laser energy diffusion, the thermodynamics and the diffusion equation itself.

2. Thermal Diffusion and Boundary Conditions

The diffusion of heat in a solid is given by the thermal diffusion equation

$$c\rho\frac{\partial T}{\partial t} - K\nabla^2 T = 0 \quad (1)$$

where: T = temperature at (x,y,z,t)

t = time

ρ = density of the solid

c = specific heat capacity of the solid

K = thermal conductivity of the solid

∇^2 = Laplacian operator

In a number of cases, one can simplify the diffusion Eq(1) to diffusion in one dimension.

Thus,

$$c\rho \frac{\partial T}{\partial t} - K \frac{\partial^2 T}{\partial x^2} = 0 \quad (2)$$

For a one-dimensional irradiation say, with a laser beam, one can further approximate the situation as an energy stream flowing into a semi-infinite solid.

Two boundary conditions are to be satisfied in such a case. One is that at the far end of the solid, there will be no temperature rise, i.e.,

$$T = 0 \quad (3)$$

when $x \longrightarrow \infty$

Here and in Eq (2), T will from now on denote the temperature rise, i.e., the initial temperature of the solid is taken to be constant with respect to time t and position x . The other boundary condition is that at the surface of irradiation. One way of tackling the problem is simply to equate the energy flux density of the irradiation to the expression of heat flow at the surface inside the solid,

$$\Phi_0 = -K \frac{\partial T}{\partial x} \Big|_{x=0} \quad (4)$$

at $x = 0$.

We will call this the constant surface heat flux solution¹⁻³.

Theory of differential equations then says that Eq (2) together with the boundary conditions (3) and (4) will determine the values of T at any space-time point (x,t) . The physical properties of the material of the solid K, c and ρ enter into the problem via Eq (2).

3. Boundary Conditions for an Irradiating Laser Beam

For irradiation with a laser beam, equating the energy flux of the beam to the heat flow is not very convincing. For example, if the solid is transparent for that particular radiation, there is then no energy absorption from the beam, and hence there will be no temperature rise. Thus, absorption has to be taken into consideration.

For a medium with an absorption coefficient α , the beam with energy flux density Φ_0 passing through it will be attenuated as:

$$\frac{\partial \Phi}{\partial l} = -\alpha \Phi \quad (5)$$

or

$$\Phi = \Phi_0 e^{-\alpha l} \quad (6)$$

for the path length l .

The energy absorbed will eventually turn into heat in the medium. The thermal diffusion equation, instead of Eq(1), will then be:

$$c\rho \frac{\partial T}{\partial t} = K \nabla^2 T + Q \quad (7)$$

where Q is the energy absorbed per unit volume per unit time, or in the one dimensional case,

$$c\rho \frac{\partial T}{\partial t} = K \frac{\partial^2 T}{\partial x^2} - \frac{\partial \Phi}{\partial x} \quad (8)$$

or

$$\frac{\partial^2 T}{\partial x^2} - \frac{1}{\kappa} \frac{\partial T}{\partial t} = -\frac{\alpha \Phi_0}{K} e^{-\alpha x} \quad (9)$$

where $\kappa = \frac{K}{\rho c}$ is the thermal diffusivity of the solid.

The boundary condition at the far end will be the same as before,

$$T = 0 \quad (10)$$

when $x \rightarrow \infty$.

At the surface of irradiation, there is no heat flow

$$-K \frac{\partial T}{\partial x} = 0 \quad (11)$$

at $x = 0$.

4. The Zero Surface Heat Flux Solution

Eq (11) is at variance with the boundary condition Eq (4). In order to appreciate the meaning of these two different formalisms, one may want to see how Eq (8) or (9) is arrived at. This will be given in another report together with its solution. For now, we write down the solution of Eq (9) with boundary conditions (10) and (11) as follows (Φ_0 is the energy flux density of the laser beam):

$$\begin{aligned} T(x, t) = & \frac{2\Phi_0}{K} \sqrt{\kappa t} \cdot \text{ierfc} \frac{x}{2\sqrt{\kappa t}} - \frac{\Phi_0}{K\alpha} \cdot e^{-\alpha x} \\ & + \frac{1}{2} \frac{\Phi_0}{K\alpha} \cdot e^{\alpha^2 \kappa t - \alpha x} \cdot \text{erfc} \left[\alpha \sqrt{\kappa t} - \frac{x}{2\sqrt{\kappa t}} \right] \\ & + \frac{1}{2} \frac{\Phi_0}{K\alpha} \cdot e^{\alpha^2 \kappa t + \alpha x} \cdot \text{erfc} \left[\alpha \sqrt{\kappa t} + \frac{x}{2\sqrt{\kappa t}} \right] \end{aligned} \quad (12)$$

where

$$\text{ierfc} y = \int_y^\infty \text{erfc} t dt \quad (13)$$

and $\text{erfc} t$ is the complimentary error function

$$\text{erfc} t = \frac{2}{\sqrt{\pi}} \int_t^\infty e^{-u^2} du = 1 - \text{erf} t \quad (14)$$

$$\text{erf} t = \frac{2}{\sqrt{\pi}} \int_0^t e^{-u^2} du \quad (15)$$

For irradiation of duration τ , the temperature rise for $0 < t < \infty$ will be given by

$$\Delta T = U(t) \cdot T(x, t) - U(t - \tau) \cdot T(x, t - \tau) \quad (16)$$

where $T(x,t)$ is the function $T(x,t)$ given by Eq. (12), and $U(t), U(t-\tau)$ = Heaviside functions at t and $t-\tau$.

In the original solution^{4,5} (no derivation was given) of Eq (12) a factor α in the denominator of their third term was missing⁴. We verified that Eq (12) is the correct solution.

5. Computations for a Skin Simulant - Long Duration Pulse

With the aid of a computer, the solution Eq (12) and Eq. (16), can be computed for different cases. For skin simulant, the results obtained may be characterized by two groups: (1) with exposure to the laser from a few seconds to say 10 milliseconds and (2), from a few milliseconds to 20 microseconds. Figs. 1 and 2, with exposure time $\tau = 10$ seconds and 0.5 second, show the typical heating characteristics of the exposures to the longer duration pulses. The curves in both figures are the temperature rise curves at depth $x = 0, 40, 80, 120$ and $160\mu m$, with $\Phi_0 = 0.167 \frac{cal}{cm^2 s}$, $K = 1.16 \times 10^{-3} \frac{cal}{cm^2 s^0 C}$, $\kappa = 1.11 \times 10^{-3} \frac{cm^2}{s}$, and $\alpha = 840 cm^{-1}$.

One notes in Fig. 2 the peaks occur from $\frac{t}{\tau} = 1.0$ at $x = 0$, to $\frac{t}{\tau} \approx 1.5$ at $x = 160\mu m$, and the pulse shape is broadened as the temperature wave penetrates into the material (skin). This is indeed the case, as we remember that the temperature wave propagates with a velocity depending on the frequency of the temperature source and hence one will see the dispersion or the broadening of a driving pulse.

The occurrence of the temperature peaks at various depths in Fig. 2 is shown in Table 1.

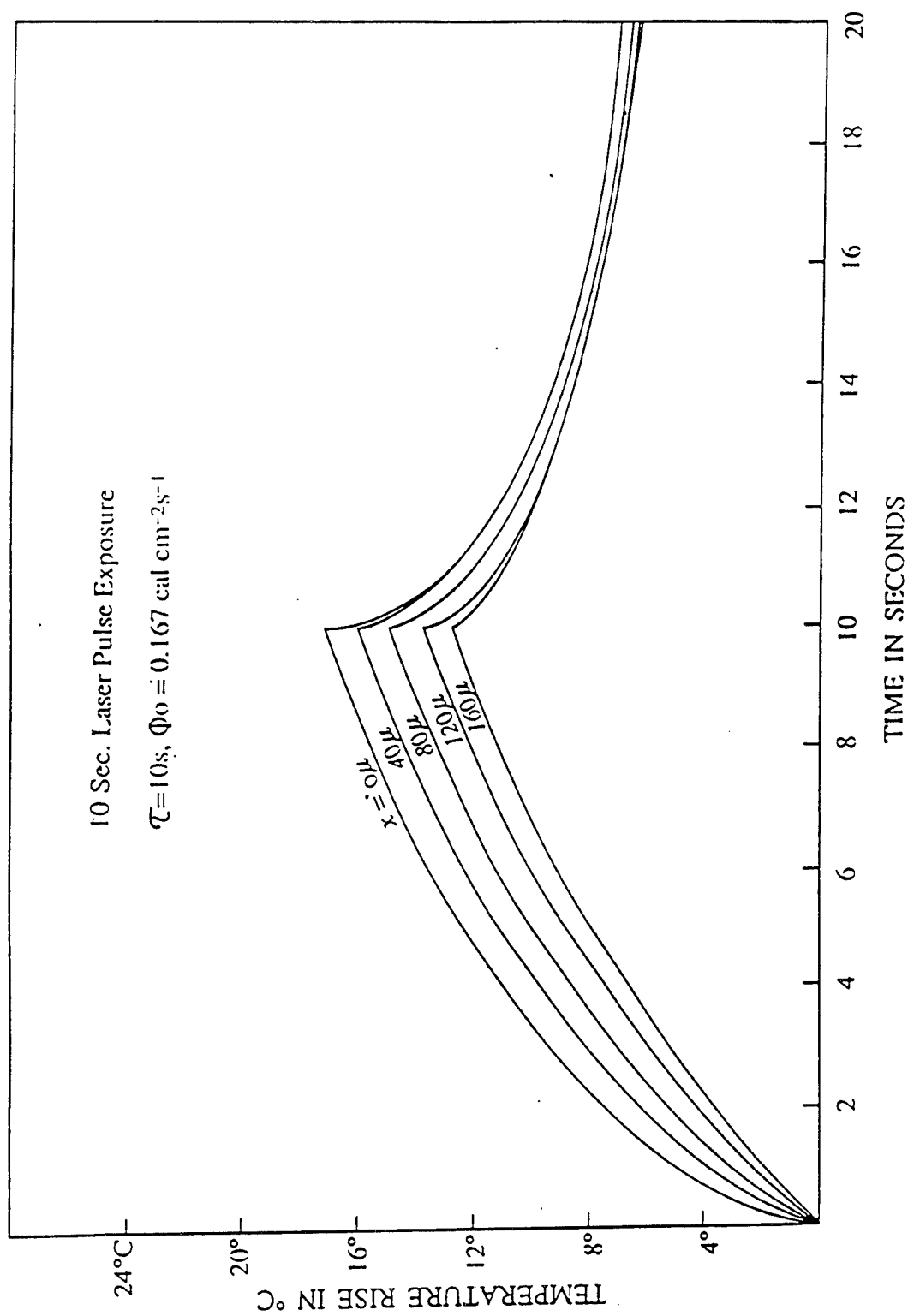


Figure 1. Temperature rise curves of skin simulant exposed to a laser pulse of $\tau = 10s$, $\Phi_0 = 0.167 \text{ cal cm}^{-2} s^{-1}$ at depths $x = 0, 40, 80, 120$ and $160 \mu m$

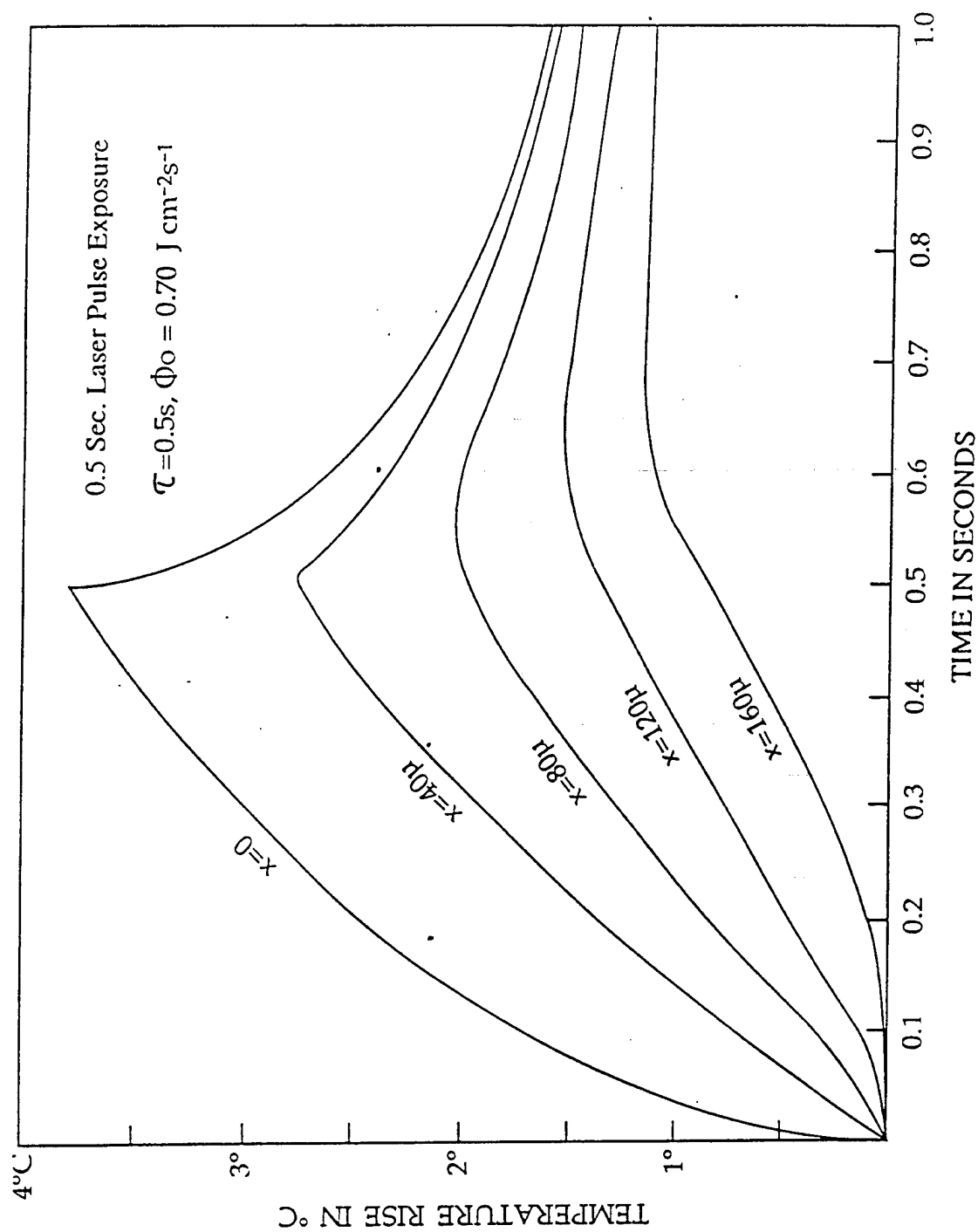


Figure 2. Temperature rise curves of skin simulant exposed to a laser pulse of $\tau = 0.5s$, $\Phi_0 = 0.167 \text{ cal cm}^{-2} \text{ s}^{-1}$ at depths $x = 0, 40, 80, 120$ and $160 \mu m$

Table 1

**TEMPERATURE PEAKS AT VARIOUS DEPTHS OF SKIN
SIMULANT EXPOSED TO LASER PULSE OF $\tau = 0.5S$ AND $\Phi_0 = 0.167$**

$$\frac{CAL}{CM^2S}$$

Depth x (microns)	Time of Peak $\frac{t}{\tau}$
0	1.0
40	1.02
80	1.10
120	1.30
160	1.50

6. Millisecond and Microsecond Pulses - Differences in the Two Formulations and the Depths of Penetration

We now turn to irradiation of short pulses.

(a) 1 Millisecond Pulse

With a 1 ms pulse and energy flux density $\Phi_0 = 40 \text{ cal cm}^{-2}\text{s}^{-1}$, the surface temperature rise at the end of the pulse is 18.8°C , and at $x = 40\mu\text{m}$, the temperature rise is 1.7°C . These are the two points plotted in Fig.3 joined by the heavy solid line (1). With $\Phi_0 = 16.7 \text{ cal cm}^{-2}\text{s}^{-1}$, the surface temperature rise is 7.9°C , and at depth

$x = 40\mu m$, the temperature rise is $0.7^\circ C$. These are joined by the heavy dashed line (2) in the figure. These are the temperature rise values calculated from Eq (12), i.e., from the heat diffusion equation Eq. (9) with zero heat flux boundary condition Eq (11) at $x=0$. The corresponding values at $x=0$ and $40\mu m$ given by diffusion equation Eq. (2) and the constant heat flux boundary condition Eq. (4) at $x = 0$ are $41.0^\circ C$ and $0.1^\circ C$ respectively, for $\Phi_0 = 40 \text{ cal cm}^{-2}s^{-1}$ (light solid lines (1') in Fig 3); and $17.1^\circ C$ and $0.05^\circ C$ respectively for $\Phi_0 = 16.7 \text{ cal cm}^{-2}s^{-1}$ (light dashed line (2') in Fig.3).

The conventions of the lines plotted here and in the following figures are: Solutions with zero surface heat flux boundary condition are plotted in heavy solid lines (labeled as (1)) and heavy dashed lines (labeled as (2)), solid lines for $40 \frac{\text{cal}}{\text{cm}^2 s}$ flux density, and dashed lines for $16.7 \frac{\text{cal}}{\text{cm}^2 s}$. Solutions with constant surface heat flux boundary conditions are plotted in light solid lines (1'), and light dashed lines (2'), again, solid lines for $40 \frac{\text{cal}}{\text{cm}^2 s}$ flux density, and dashed lines for $16.7 \frac{\text{cal}}{\text{cm}^2 s}$.

It is to be noted that the values of the temperature rise, both at the surface and underneath, given by the conventional constant surface heat flux formalism of Eqs (2), (3) and (4), are higher than that by the more realistic and logical consideration of Eqs. (9), (10) and (11), i.e., the zero surface heat flux solution (12). In fact, as the laser pulses become shorter and shorter, the difference becomes larger and larger, and, as will be seen below, with a $20\mu s$ laser pulse, the constant heat flux formalism gives values ten times higher than that given by zero surface heat flux solution (12). In the meantime, solution (12) shows that the laser beam penetrates much deeper than that predicted by Eqs (2), (3) and (4). For exposures of seconds duration, the difference given by the two formalisms is small and may be neglected for all practical purposes.

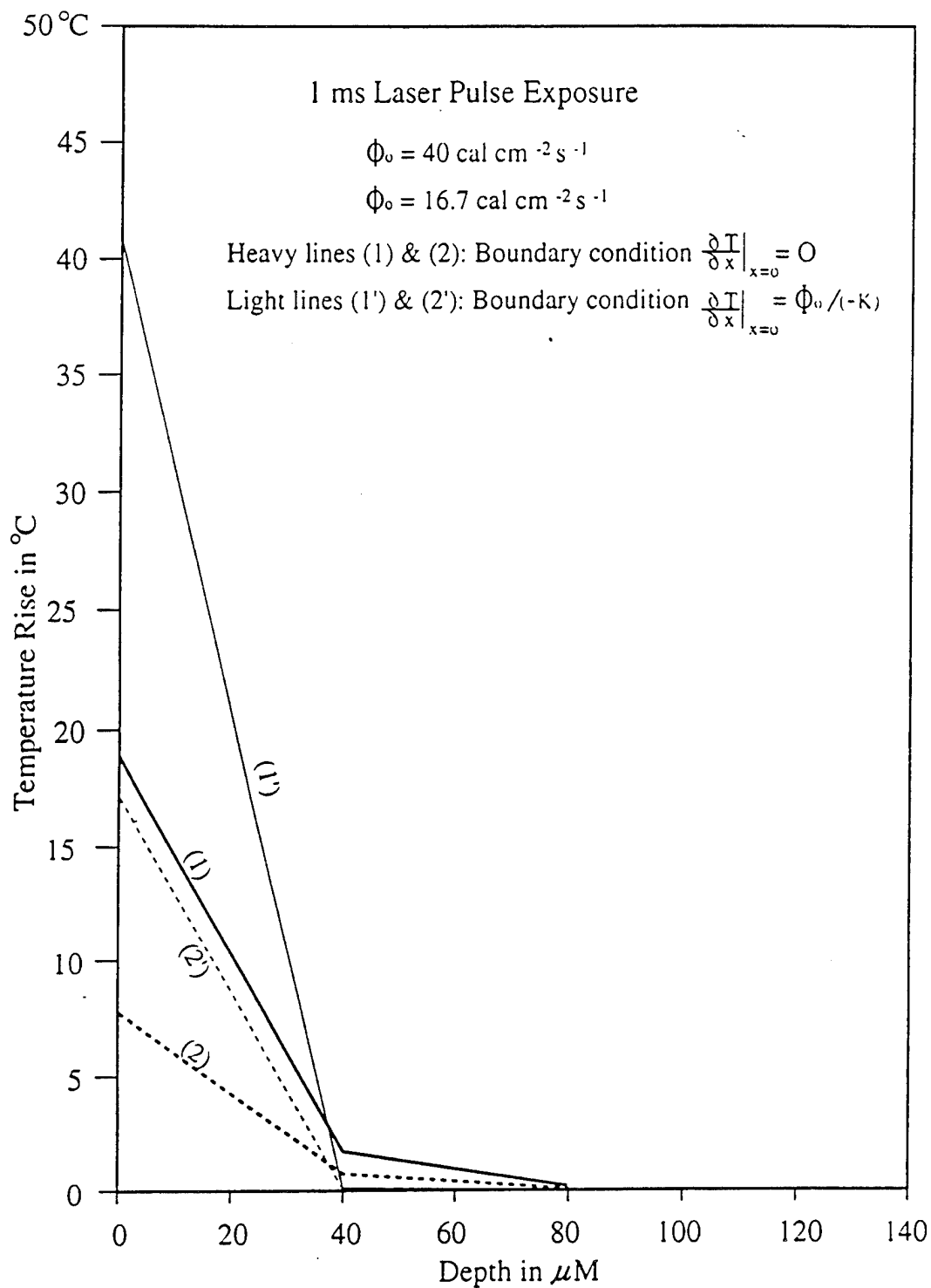


Figure 3. Temperature rise of skin simulant at depths $x = 0, 40$, and $80 \mu\text{m}$ for laser exposure of $\tau = 1\text{ms}$, $\Phi_0 = 40$ and $16.7 \text{ cal cm}^{-2} \text{ s}^{-1}$. Heavy lines are with $\partial T / \partial x|_{x=0} = 0$, light lines with $-K \partial T / \partial x|_{x=0} = \Phi_0$ boundary conditions. The figure shows the much higher surface temperature rise of a solid given by the constant surface heat flux solution

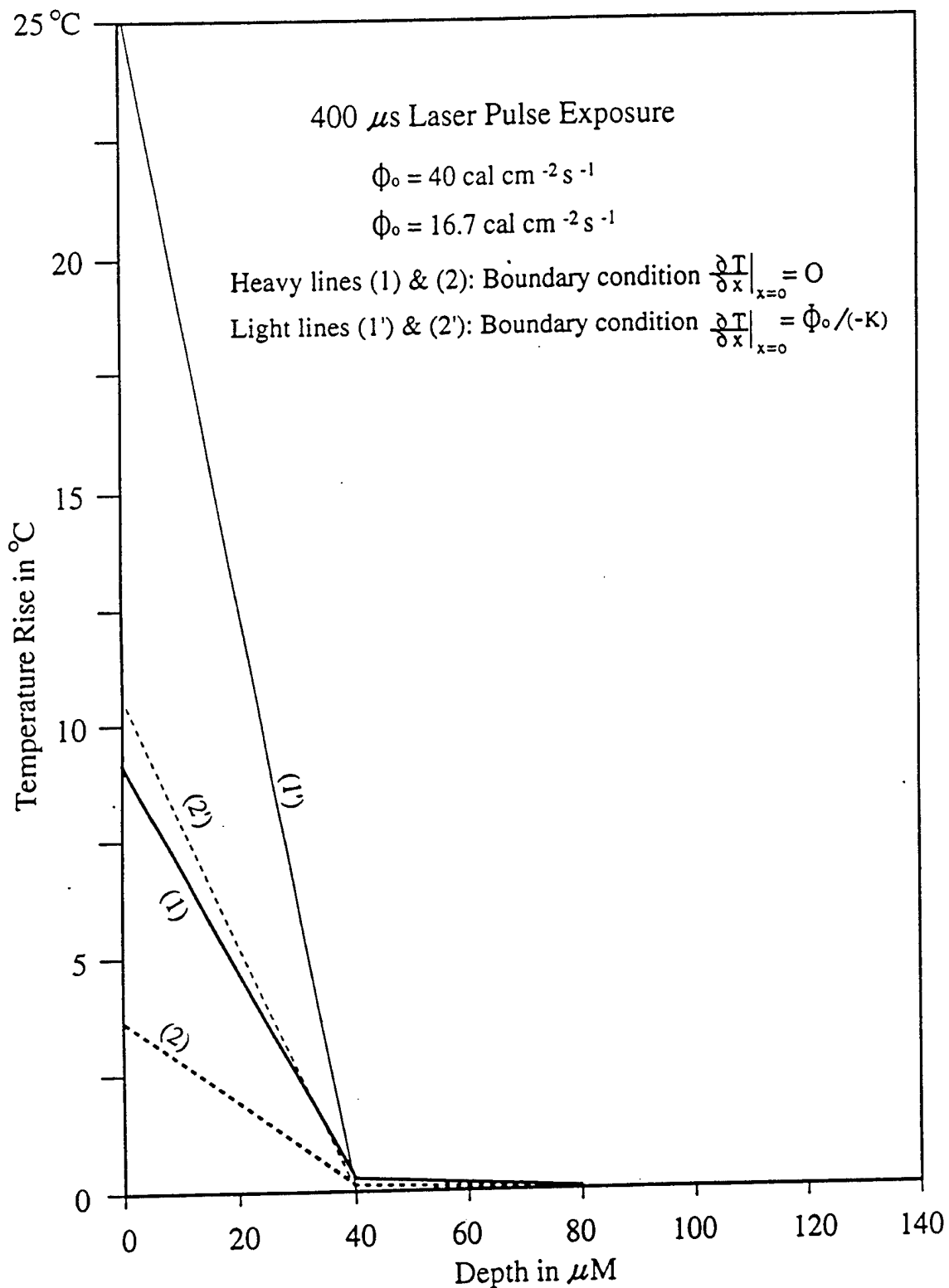


Figure 4. Temperature rise of a skin simulant at depths $x = 0, 40$, and $80 \mu\text{m}$ for laser exposure of $\tau = 400 \mu\text{s}$, $\Phi_0 = 40$ and $16.7 \text{ cal cm}^{-2} \text{ s}^{-1}$. The figure shows the much higher surface temperature rise of a solid given by the constant surface heat flux solution.

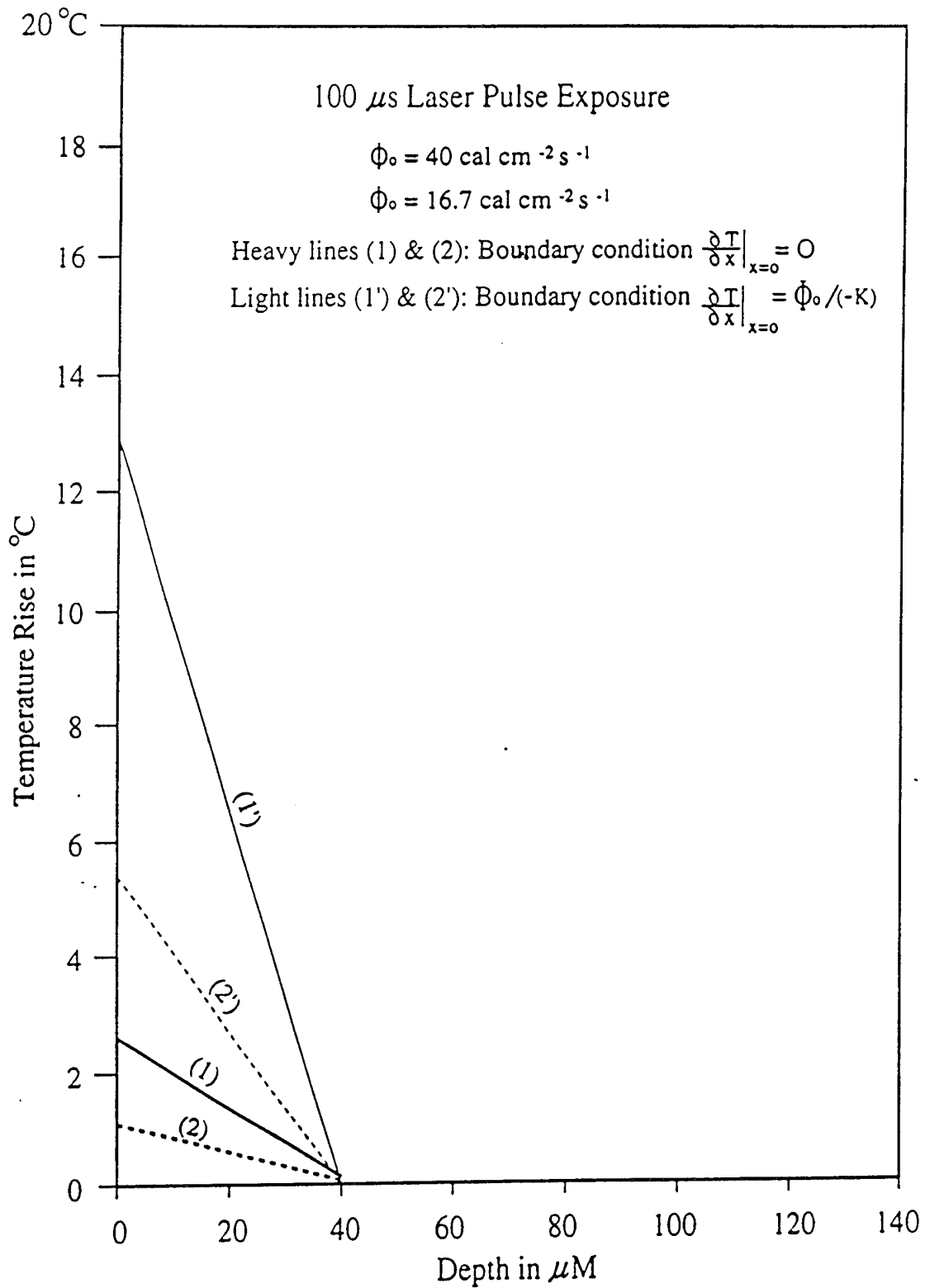


Figure 5. Temperature rise of a skin simulant at depths $x = 0, 40$, and $80 \mu\text{m}$ for laser exposure of $\tau = 100 \mu\text{s}$, $\Phi_0 = 40$ and $16.7 \text{ cal cm}^{-2} \text{ s}^{-1}$. The figure shows the much higher surface temperature rise of a solid given by the constant surface heat flux solution.

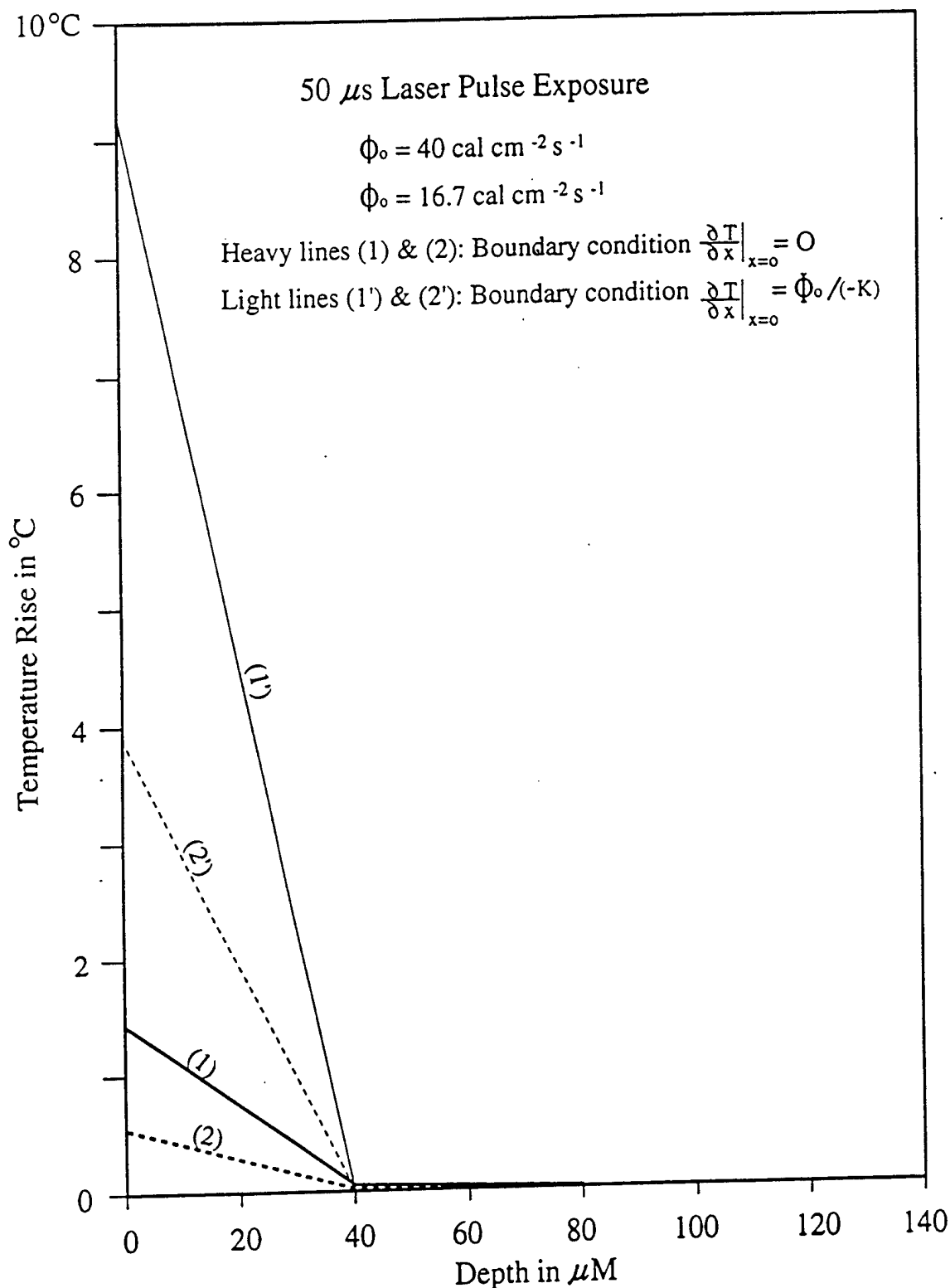


Figure 6. Temperature rise of a skin simulant at depths $x = 0, 40$, and $80 \mu\text{m}$ for laser exposure of $\tau = 50 \mu\text{s}$, $\Phi_0 = 40$ and $16.7 \text{ cal cm}^{-2} \text{ s}^{-1}$. The figure shows the much higher surface temperature rise of a solid given by the constant surface heat flux solution.

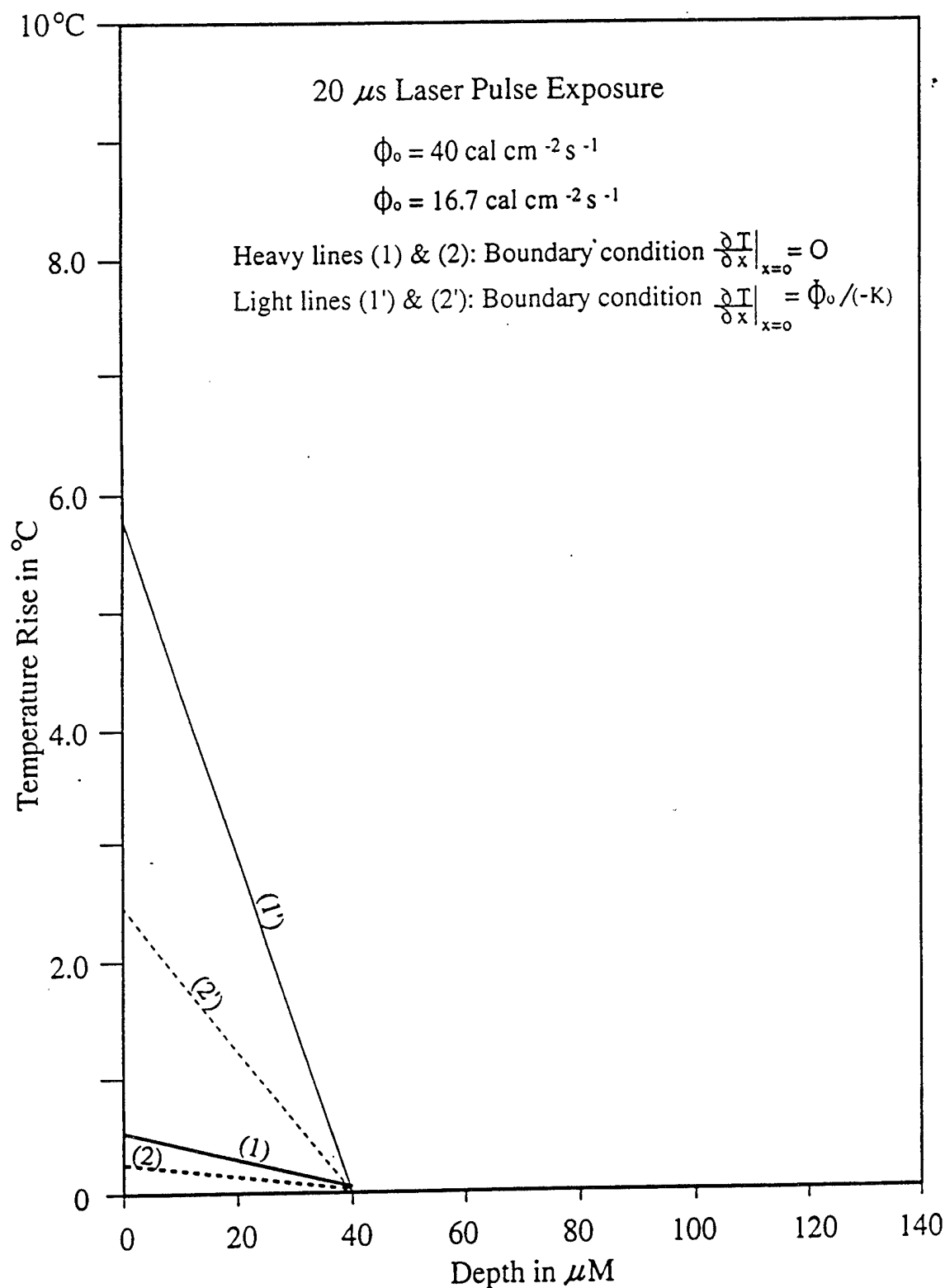


Figure 7. Temperature rise of a skin simulant at depths $x = 0, 40, \text{ and } 80 \mu\text{m}$ for laser exposure of $\tau = 20 \mu\text{s}$, $\Phi_0 = 40 \text{ and } 16.7 \text{ cal cm}^{-2} \text{ s}^{-1}$. The figure shows the much higher surface temperature rise of a solid given by the constant surface heat flux solution.

(b) 400 μ s Pulse

For 400 μ s pulse of the same energy flux density $\Phi_0 = 40 \text{ cal cm}^{-2}\text{s}^{-1}$, the temperature rise calculated from Eq (12) at the surface is 8.9°C; at $x = 40\mu\text{m}$, 0.5°C; and at $x = 80\mu\text{m}$, 0.02°C (joined by the heavy solid lines in Fig 4). For $\Phi_0 = 16.7 \text{ cal cm}^{-2}\text{s}^{-1}$ at depths $x=0$, 40 μm and 80 μm , T is 3.7°C, 0.2°C and 0.009°C respectively (heavy dashed lines (2) in Fig 4).

Calculated from diffusion equation (2) and boundary condition (4) at $x=0$, the corresponding values for $\Phi_0 = 40 \text{ cal cm}^{-2}\text{s}^{-1}$ are 25.4°C at $x=0$ and $1.5 \times 10^{-4}\text{C}$ at $x = 40\mu\text{m}$ (joined by light solid lines (1'), Fig 4); and for $\Phi_0 = 16.7 \text{ cal cm}^{-2}\text{s}^{-1}$, 10.8°C and $6.4 \times 10^{-5}\text{C}$ at $x=0$ and 40 μm respectively (joined by light dotted line (2') in Fig 4). At 80 μm , the temperature rises are zero ($\sim 10^{-17}\text{C}$) for both energy flux densities Φ_0 , and are not plotted in the Figure.

(c) 100 μ s, 50 μ s and 20 μ s Pulses

The results given by the two formalisms for these short μ s pulses and the same energy flux densities $\Phi_0 = 40 \text{ cal cm}^{-2}\text{s}^{-1}$ and $16.7 \text{ cal cm}^{-2}\text{s}^{-1}$, are shown in Tables 2 and 3 along with those of 1 ms and 400 μ s exposures. They are similarly plotted in Figs 5, 6 and 7.

7. Discussion

As remarked above, the constant surface heat flux solution gives much too high a temperature rise at and near the surface: For a ms pulse, it is higher by a factor of 41.0/18.9 or ≈ 2.2 ; for a 400 μ s pulse, by a factor of 2.8; for a 100 μ s pulse, by a factor of 4.9; for a 50 μ s pulse, by a factor of 6.6; and for a 20 μ s pulse, by a factor of 9.8, than that given by the zero surface heat flux solution. On the other hand, the depth of penetration of the laser pulse by the constant surface heat flux solution becomes smaller and smaller as the pulse width decreases. This behavior as depicted by the

TABLE 2
TEMPERATURE RISE BY THE TWO DIFFERENT BOUNDARY
CONDITIONS* $\Phi_0 = 40 \frac{\text{cal}}{\text{cm}^{-2}\text{s}}$

τ	x in μM	$\Phi_0 = 40 \text{ cal cm}^{-2}\text{s}^{-1}$	
		$(\frac{\partial T}{\partial t} _0 = 0)$	$(\frac{\partial T}{\partial x} _0 = -\Phi_0/K)$
1 ms	0	18.9C	41.0C
	40	1.69	0.12
	80	0.06	7.2×10^{-7}
400 μs	0	8.93	25.4
	40	0.53	1.5×10^{-4}
	80	0.02	0
100 μs	0	2.64	13.0
	40	0.12	0
	80	0.004	0
50 μs	0	1.39	9.17
	40	0.06	0
	80	0.002	0
20 μs	0	0.59	5.80
	40	0.02	0
	80	8.0×10^{-4}	0

* Column 3 is plotted as (1) in Figs 3-7

* Column 4 is plotted as (1') in Figs 3-7

TABLE 3
TEMPERATURE RISE BY THE TWO DIFFERENT BOUNDARY
CONDITIONS* $\Phi_0 = 16.7 \frac{\text{cal}}{\text{cm}^2 \text{s}}$

τ	x in μM	$\Phi_0 = 16.7 \text{ cal cm}^{-2} \text{s}^{-1}$	
		$(\frac{\partial T}{\partial t} _{x=0})$	$(\frac{\partial T}{\partial x} _{x=0} = \Phi_0/K)$
1 ms	0	7.98C	17.1C
	40	0.71	0.05
	80	0.03	3.0×10^{-7}
400 μs	0	3.73	10.6
	40	0.22	6.4×10^{-5}
	80	0.008	0
100 μs	0	1.10	5.42
	40	0.05	0
	80	1.7×10^{-3}	0
50 μs	0	0.58	3.83
	40	0.02	0
	80	8.4×10^{-4}	0
20 μs	0	0.25	2.42
	40	.01	0
	80	3.3×10^{-4}	0

* Column 3 is plotted as (2) in Figs 3-7

* Column 4 is plotted as (2') in Figs 3-7

constant surface heat flux solution is not surprising. In fact, the constant surface heat flux boundary condition holds only in the ideal case in which the surface of the solid

is in contact with a constant temperature heat reservoir whose temperature follows in every small (infinitesimal) step the surface temperature rise of the solid or, in the case of irradiation, when the beam energy (laser) is totally converted to heat at the surface^{6,7}. The penetration of heat in the latter case is due to diffusion given by Eq. 2 and controlled by the diffusion coefficient $\kappa = \frac{K}{\rho c}$. It is to be noted that although in the figures (Figs 3 - 7), the temperature rise versus depth graphs are all drawn as straight lines, they are actually concave .

8. CONCLUSION

The investigation of energy diffusion from a laser beam in a solid has produced many useful results related to personnel protection against such radiation and many other applications of the laser. It was presented also with the fundamental questions regarding the boundary conditions of the diffusion equations, the zero surface heat flux vs the constant surface heat flux, $\frac{\partial T}{\partial x} |_{x=0} = 0$ vs $-K \frac{\partial T}{\partial x} |_{x=0} = \Phi_0$, at the boundary. The constant surface heat flux boundary condition in the conventional solution of the heat diffusion equation is shown to be unrealistic for a laser beam. Justification for zero surface heat flux boundary condition for the laser irradiation is presented along with the calculations for the temperature rise of a skin simulant exposed to the laser irradiation. The former, (constant surface heat flux) solution gives the temperature rise higher by a factor of 2.2, 2.8, 4.9, 6.6 and 9.8, for laser exposure of 1000, 400, 100, 50 and 20 μs , respectively, than that given by the diffusion equation with zero surface heat flux boundary condition. The analysis holds for the general case of other laser irradiated solids.

REFERENCES

1. H.S. Carslaw and J.C. Jaeger, Conduction of Heat in Solids, 2nd ed., Oxford University Press, 1959, § 2.9.
2. Equation by K. Buettner quoted by John A. Weaver and Alice Stoll, Mathematical Model of Skin Exposed to Thermal Radiation, Aerospace Medicine, January, 1969, pp 24-26.
3. J.M. Davies, Skin Simulants for Studies of Protection against Intense Thermal Radiation, Review of Scientific Instruments, vol 41, 1020-1049, 1970.
4. Equation by A.J. Vendrik in H.F. Cook, A Physical Investigation of Heat Production in Human Tissues when Exposed to Microwaves, British Journal of Applied Physics, 3, 1-6, 1952.
5. Carslaw and Jaeger (Ref 1) gave the solution for heat generated inside the solid with no heat flow through the surface. The boundary condition is zero flux at the surface, ie. Eq (10).
6. Arnold Sommerfeld, Thermodynamics and Statistical Mechanics, Academic Press, 1956.
7. Arnold Sommerfeld, Partial Differential Equations in Physics, Academic Press, 1956. Sommerfeld discussed the case of Stefan-Boltzmann radiation law. It is clear that the constant heat flux boundary condition implied that the radiation was absorbed and converted to heat energy in the first few boundary layers of the material body.